CONSTRUCTION STATUS OF XFEL/SPRING-8*
(ITS STABILITY ISSUE)

Yuji Otake*, on behalf of the members of the XFEL/SPring-8 Project,
XFEL Joint Project of RIKEN/JASRI,
1-1-1 Kouto, Sayo-cho, Sayo-gun, Hyogo, 679-5148, Japan.

Abstract

The method of velocity bunching in a low-β section and magnetic bunching in a high-β section with a 3000-times bunch compression factor, based on the concept of the SPring-8 compact SASE source (SCSS), is used to make a 3 kA peak current with a 30 fs pulse width for the XFEL/SPring-8. Rf phase and amplitude variations of cavities for making the bunch compression directly and sensitively reflect to fluctuation of the peak current, which is very sensitive to lasing along an undulator section. Therefore, the rf phase and amplitude fluctuation of the cavities must be low. We have developed very stable instruments for driving the cavities to ensure the stable peak current. By using the SCSS test accelerator, the stability of the developed elements, such as a klystron high-voltage power supply with a 10 ppm(rms) variation at a 45 kV PFN charging voltage, were verified, whether the elements satisfied an electron beam energy variation of 10^{-4} demanded for the XFEL/SPring-8 or not. The result of the verification showed that it almost had sufficient performance. However, the instruments are still under development to realize a further low-noise rf system and a more stable power supply, which pushes the XFEL stability higher than the design target. This report presents the construction status of the XFEL/SPring-8, and the development status of the elements.

INTRODUCTION

In institutes of several countries, an X-ray free electron laser (XFEL) as 4th-generation light sources, such as Japanese XFEL[1], European XFEL[2], and LCLS (SLAC)[3], are being constructed. They generate intensive, coherent, and extreme short-pulse light of X rays, like flash, and may open a new window of science,

such as protein structural analysis, by using single-particle analysis[4]. This light source is realized by a self-amplified spontaneous emission (SASE) principle, because of no mirror for X rays. Figure 1 shows a cartoon of an outline of the XFEL/SPring-8, and Figure 2 shows a summarized development and construction schedule of the XFEL. The basic parameters of the XFEL are listed in Table 1[5]. The development and construction schedule is mainly categorized by two phases. One is phase-I to make a proof-of-principle stage, by constructing the SPring-8 compact SASE source (SCSS) test accelerator and developing its constituent parts, such as power supplies. The next is phase-II that is for constructing the actual XFEL using an 8 GeV linac and in-vacuum undulators, as well developing the necessary components to increase its stability toward stable SASE generation. We are almost in phase-II. The outstanding point of our XFEL, based on the concept of SCSS, compared with the others is compactness[6]; that is about one third of the others in length. This short length is realized by technologies of a small emittance of 0.7 πmmmrad, achieved with a CeB6 thermionic electron gun, short-length acceleration realized with a C-band (5712 MHz) cavity having an electric field of more than 35 MV/m, and an in-vacuum undulator with a short period of 18 mm and a large K value of K_{max}=2.2. This machine concept was already proved by using the 250 MeV SCSS test accelerator in phase-I. In accordance with the SCSS concept, the bunch compression method uses velocity bunching in the low-β section between the electron gun and L-band cavities of an injector, and magnetic bunching in high-β by employing a magnetic chicane composed of four dipole magnets, as shown in Fig. 1, must be used.
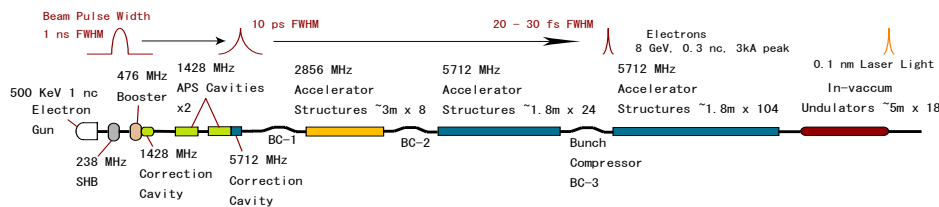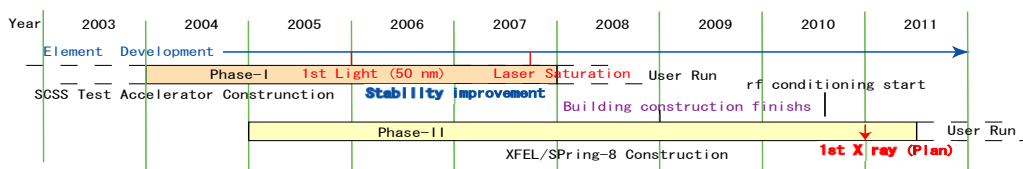

Figure 1: Configuration of XFEL/SPring-8.

Figure 2: Time table for developing and constructing the SCSS test accelerator (Phase-I) and the XFEL (Phase-II).

*otake@spring8.or.jp

X-ray FELs

Table 1. General Feature of XFEL/Spring-8 vs. the SCSS Test Accelerator

	XFEL/SPring-8 (design)	SCSS (measured)
Energy	~8 GeV	250 MeV
Charge amount	~ 0.3 nC	~ 0.3 nC
Peak current	~ 3 kA	300 A
Emittance	~ 1 πmmmrad	~ 0.7 πmmmrad
Size	~ 50 μm (rms)	~ 100 μm (rms)
Laser energy/ pulse		30 μmJ @ 60 nm
Pulse width for SASE generation	~ 40 fs (rms)	300 fs

Table 2. Tolerance of the phase and amplitude stability of each cavity.

Cavity	Δφ (deg. ms)	ΔV/V(%rms)	Δt (ps rms)
238 MHz SHB	± 0.01	± 0.01	± 0.12
476 MHz Booster	± 0.02	± 0.01	± 0.12
L-band Cor. Cavity	± 0.06	± 0.03	± 0.12
L-band APS Cavity	± 0.06	± 0.01	± 0.12
C-band Cor. Cavity	± 0.06	± 0.1	± 0.049
S-band Accelerator	± 0.1	± 0.01	± 0.097
24C-band Accel. (up-stream)	± 0.2	± 0.01	± 0.097
104 C-band Accel. (Down-stream)	± 0.5	± 0.01	± 0.24

Table 3: Achieved Stability Parameters of the SCSS Test Accelerator

Energy stability	~0.06% (rms)
Beam Current stability	10~20 % (full width)
Beam pointing stability	~ 30 μm (rms)
Laser stability (60 nm)	~ 11% (rms)
Laser pointing stability (60 nm)	~ 5% (rms) of 3mm size
Time jitter between rf and beam	~ 46 fs (rms)

This bunch compression makes a 3 kA peak current with a pulse width of 30 fs by a 3000-times bunch compression. Making fluctuation of this peck current as small as possible is very effective to obtain stable lasing of X rays along a long undulator section of 90 m at the XFEL. The peak-current fluctuation within about 10% for stable lasing was suggested by our beam-tracking simulation using the Monte Carlo method[5]. Therefore, the rf phase and amplitude stabilities of the rf cavities for these-bunch compression sections are very important, especially in the injector, because the phase and amplitude fluctuation makes the peak-current fluctuation, which directly connects to the X ray lasing fluctuation. These acceptable stabilities were also calculated by the simulation as shown in Table 2. From knowledge based on operation experience in the test accelerator and the above-mentioned simulation results, we found out what we had to do in phase-II to realize the XFEL having very stable light. The target performance of the next component development to serve the performance listed in Table 2, such as allowable high-voltage stability for a klystron and acceptable noise and drift of an rf signal, was decided. This paper describes the achieved performance, the details of the target performance, the development status of the accelerator components including an enclosing building to maintain an environmental temperature at constant, and some results of experiments to evaluate the components.
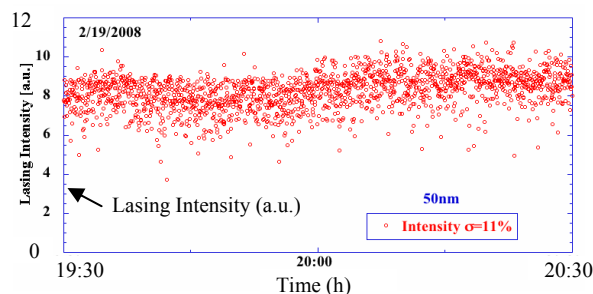
X-ray FELs

Figure 3: Stability of the SASE lasing intensity over 1 hr with 10 Hz repetition. The lasing wavelength is 50 nm.
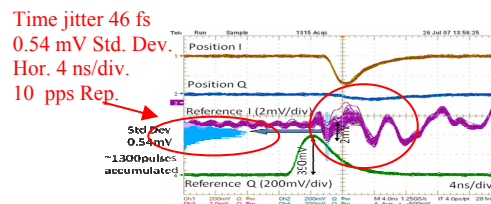

Figure 4: Beam arrival time jitter measured with the BPM intensity detection cavity; 1300 pulses accumulated.

ESTABLISHED AND DEMADED PERFORMANCE

Established stability at the SCSS test accelerator to proof XFEL feasibility

- Laser performance

Laser light (60 nm) with a saturated state of SASE non-linear amplification at the SCSS test accelerator was continuously generated with an energy of 30 μJ, a pulse width of 300 fs, and a fluctuation of 11% (rms) for more than one hour, as shown in Fig. 3. The laser pointing stability was less than 5% of 3 mm (FWHM) in size, and its spectrum width was 0.6% (FWHM, average). These laser performances are tabulated in Table 3[7].

- Electron beam performance

The features of an electron beam at the accelerator are as follows. For example, a beam emittance of 0.7 πmm mrad was evaluated by comparing the data between the measured lasing intensity in accordance with changing K-values and SIMPLEX simulations[6]. The time jitter between an electron beam and the acceleration rf was 46 fs (STD, Fig. 4), which was measured with the phase and intensity reference cavity of a TM110 mode cavity-type beam-position monitor (BPM)[8]. The pointing stability of the beam was about 30 μm (rms), which was also observed with the BPM. The beam energy stability was less than 0.06% (full width). These data are tabulated in Table 3. To achieve this stability, there were big improvements related to sub-harmonic buncher (SHB) cavities in the injector of the test accelerator[9] and the high-voltage stability of inverter power supplies for a klystron[10] and an induction output tube (IOT) as an rf source of the 476 MHz SHB in the injector.

- Technology to support rf stability

The improvement was that the rf phase and the amplitude drift of the 238 MHz SHB was decreased up to 0.02 deg. (rms) and 0.03% (rms), as shown in Fig. 5. This result was achieved by increasing the setting accuracy of the rf phase and amplitude on an IQ controller with instrumental temperature regulation within +/- 0.1 K, and decreasing the temperature drift of the 238 MHz and 476 SHBs. This controlled small drift was realize by changing the temperature monitoring point for PID feedback control from on the SHB body surface to its cooling water inlet. The achieved temperature stability was about 0.01 K (STD).[9,11]
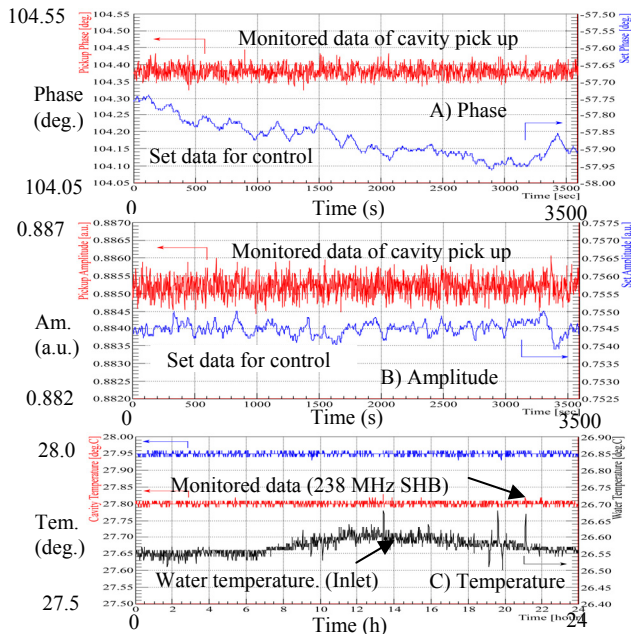

Figure 5: Stabilities of the 238 MHz SHB cavity. Phase (upper), amplitude (middle), and cavity temperature (lower).
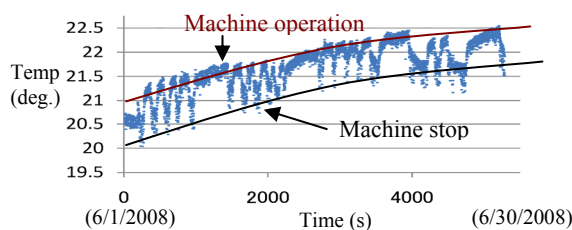

Figure 6: Temperature stability of the accelerator tunnel at the SCSS test accelerator. The steep up/down of the graph's line shows a cyclic day-by-day operation.

- Technology to support high-voltage stability

Another improvement was decreasing the high-voltage jitter of the 45 kV inverter power supply for the klystron[10] from about 0.02% (rms) to about 0.002% (rms). This voltage jitter performance was achieved with combined inverter power supplies, including a 20 kHz switching main power supply for rough voltage control and an 80 kHz auxiliary power supply for precise voltage control, which expands the response frequency bandwidth of the feedback control. Furthermore, the high-voltage jitter of the 38 kV inverter power supply for the IOT

also refined up to 0.06% (rms) by optimizing its voltage feedback control parameters.

- Technology to support environmental temperature stability

To obtain good temperature stability in an accelerator tunnel having a 1.5 m thick concrete wall, no equipment of an air conditioner was recommended, because of a big perturbation from the air conditioner control. In the case of the test accelerator, the temperature variation in the tunnel was +/- 1 K for one month, without the air conditioner, as shown in Fig. 6. This temperature change was mainly due to the temperature variation of the cooling water for the accelerator, and was strongly affected by the thermal-shield effect of the wall. However, since the temperature in the klystron gallery of the test accelerator was sometime controlled over about 4 K from the average temperature in the worst case, this variation had an unstable effect on the lasing of the test accelerator.

Stability demanded for accelerator components

The rf amplitude and the time stability needed to attain an energy stability of 10^{-4}, demanded for the XFEL, was calculated by a simulation, as shown in Table 2[5]. By comparing the stability between those of the test accelerator and the XFEL, the factor two or three of difference between them must be improved. To achieve stability for the XFEL, the fundamental technologies, as mentioned below, are especially important. These fundamental technologies are the small-amplitude ripple at the output of a high-voltage power supply for a klystron, and the low-phase jitter of an rf signal to drive the klystron, due to noise, and the lower thermal drift of the rf signal and other components.

- High-voltage stability required for the klystron

The relation between the high-voltage, V_k, and the klystron output power, P_{rf}, is expressed by the equation

$$P_{rf} = \eta\, I_k\, V_k = \eta\, k\, V_k^{2.5}, \qquad\qquad 1)$$

where η is the conversion efficiency of a klystron, I_k is the klystron cathode current, and k is the klystron perveance[12]. The demanded high-voltage stability was roughly estimated by a calculation based on this equation using the required energy stability of 10^{-4}. The estimated stability was less than 100 ppm (full width). This voltage stability is almost applied to all rf sources that use vacuum tubes, such as the klystron and IOT.

- Demanded rf signal stability

The short-period stability of the rf signal with a frequency of more than 100 Hz is mainly due to side-band noise around an rf carrier signal. In addition, the rf power fluctuation of below 100 Hz is removed by feedback control. The electron beam in an acceleration cavity feels an electric field generated by the rf signal, including the noise. Therefore, this noise directly affects the energy fluctuation (or jitter) of the beam. Obtaining the temporal noise intensity $N(t)$ directory connected to the power fluctuation is performed by integrating the side-band noise on its frequency spectrum along a necessary bandwidth by using the equation

$$N(t) = \int w(1/f) N_{SSB}(f) df , \qquad 2)$$

where $N_{SSB}(f)$ is the side-band noise, f is the frequency and $w(1/f)$ is the weight function[13,14]. The obtained temporal noise intensity is the worst case of the energy fluctuation, when all noise components coherently affect the beam acceleration. The necessary bandwidth for the integration is approximately determined by a triangle weight function of $w(1/f)$, which is the result of pulse modulation of an rf signal. This bandwidth is approximately from 10 kHz to 10 MHz. When assuming that the required beam energy fluctuation is 10^{-4}, and an rf pulse width of 1 μs, -120 dBc average noise level on the frequency spectrum within the bandwidth is needed to avoid any apparent fluctuation of the beam energy.

- Environmental temperature stability required for accelerator instruments

From the viewpoint of the thermal dependence on the accelerator components, it is not easy to evaluate, because there are many components having thermal dependence, such as rf cables being passive devices and power supplies being active devices. However, we can only say that the variation of the environmental temperature should be as small as possible for stably generating SASE. To show a criterion of the thermal variation effect to the accelerator instruments, an rf cable case is a typical example. Phase-stabilized rf cables are used in the SCSS test accelerator, and will also be employed in the XFEL. This cable (HF-15D) has a thermal electrical length coefficient of 8 ppm/K, and could be improved by up to 3 ppm/K for our demand by HITACH Cable Corporation. If 10 m long of the rf monitor cable with 8 ppm/K, which is laid down from a 5712 MHz travelling-wave tube to an instrumentation rack, is assumed, the phase variation is 0.55 deg./K (255 fs/K). This value is about ten-times larger than that tabulated in Table 2. It is not allowable, if the requirement is considered. Of course, there are other kinds of effects. Even if we only consider the rf cable effect, the environmental temperature should be controlled to within 0.1 K to satisfy the demand.

FURTHER COMPONENT DEVELOPEMTS TOWERD XFEL

Since there were some differences between the actually achieved stability and those given in Table 3, the stability of the components, like the power supplies and the rf source, should be improved. Therefore, further improvements of the components stability have been conducted as follows.

Highly accurate inverter power supply

For obtaining further output voltage regulation of the inverter power supplies, the refinement proceeded as follows. The combined inverter power supply for the klystron was originally separated into the main and auxiliary power supplies. To improve its controllability, these two power supplies were unified. To have more precise voltage control accuracy of both inverter power

supplies for the IOT and klystron, the electrical shield around a deviation amplifier for feedback control was reinforced so as to reduce noise, and its feedback parameter was optimized. By doing this voltage regulation of the power supply for the klystron was improved by up to about 0.001% (rms), as shown in Fig. 7. The high-voltage jitter of the power supply for the IOT was also refined up to 0.002% (rms).
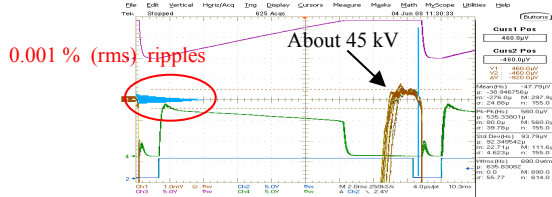

Figure 7: Voltage stability of the improved inverter power supply for the klystron of XFEL/SPring-8.
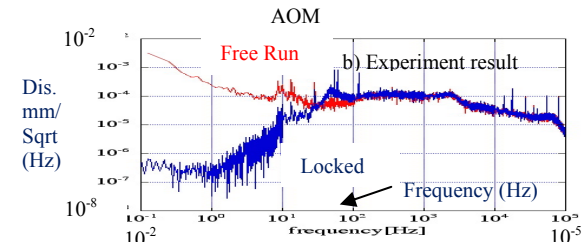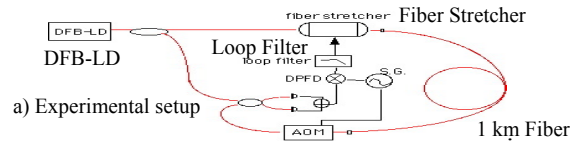

Figure 8: Experimental set up used to evaluate the optical length control of the fiber (upper), and its experiment result (lower).

Extremely precise rf driving system

There are mainly two problems, which we should overcome, to realize the time accuracy given in Table 2. One is the problem of the detection and control accuracy of an rf phase and amplitude up to 0.01 deg. at 5712 MHz. Another problem is a long distance time (rf) reference signal transmission for about 700 m of the XFEL/SPring-8. Both of these will be solved by using the 1550 nm laser and optical fiber technology, which is commonly used in telecommunications. The 0.01 deg. rf phase control and the long-distance signal transmission can be attained by the optical length control of a fiber using Micelson interferometory. An instrument using this method has been developed[8]. The developed instruments were tested by using existing 1 km optical fiber cables with a thermal optical length coefficient of 2ppm/K. The cables lay down along the circumference of the SPring-8 ring accelerator. Figure 8 shows the instrument configuration for the test and its optical length control performance. From the result, the optical length change (mainly thermal effect) of the fiber was minified up to several micron-meters for 1 km in length by the instrument. This value corresponds to several femto-seconds, and is almost satisfactory for our demand tabulated in Table 2. An optical transmitter and a receiver using a wavelength-

X-ray FELs

division multiplexing technique for transmitting optical signals combined with multi frequency signals of 5712 MHz, 2856 MHz, 1428 MHz, 476 MHz, 238 MHz, and a phase switch keying (PSK) modulated trigger pulse, has been developed as well the above-mentioned development. The result of a preliminary test for the transmitter and receiver showed their noise level was sufficiently low to almost satisfy our required time stability, given in Table 2. But, unfortunately, the rf phase detection method to guarantee femto-second accuracy is still under development.

Environmental temperature regulation

The accelerator tunnel thermal stability is probably sufficient, as mentioned above. However, the klystron gallery of the test accelerator is not enough. Therefore, the temperature condition of the klystron gallery of the XFEL should be improved. To solve this problem, we employ double-surface walls (roofs) of an enclosure building for the XFEL to equip thermal insulation. The medium layer space between the walls is ventilated with temperature-controlled air within +/- 2 K for the thermal insulation. To have more precise temperature control around the accelerator instruments, the thermally controlled 19" enclosure, as shown in Fig. 9, is employed. The inside temperature of this enclosure, having a 1 kW inner dummy heat source, was regulated to within +/- 0.2 K by its inner recirculating air, even through, the surrounding temperature of it changed by 3~4 deg.. The heat of the air was exchanged with a heat-exchanger cooled by water controlled within +/- 0.2 K in a steady state (e.g. Fig. 10).
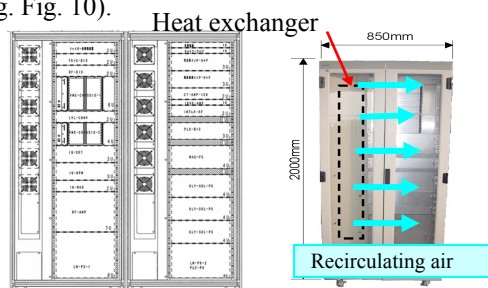

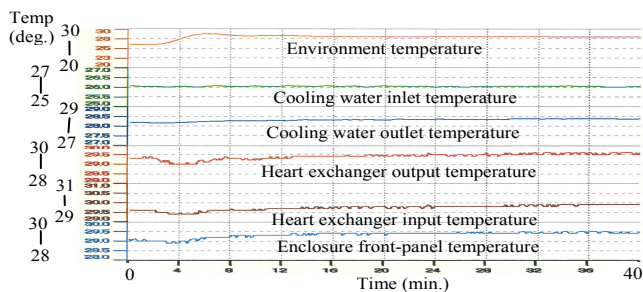
Figure 9: Thermally controlled 19" enclosure.

Figure 10: Performance of the temperature control of the 19" enclosure with a constant 1 kW heat source in it. The air in the enclosure was controlled to within a temperature of +/- 0.2 K with a water-cooled heat exchanger.

SUMMARY

We almost finished the stage of phase-I to confirm the feasibility of the XFEL/SPring-8 with the fruitful result, such as a lasing stability of 11% (rms), and checked for any inadequacy points to realize the XFEL. There were some differences between the demanded time stability and the established time stability. To make up for the difference, and to increase the possibility for stable X ray lasing, the stability of the components, such as the inverter power supply for the klystron and IOT, were improved up to a voltage regulation of less than 20 ppm (rms). For obtaining more precise rf control and for adapting long-distance rf transmission, an instrument for optical length control of the fiber was developed with a performance of its length control of several μm for 1 km. To increase the thermal stability of the environment for the XFEL, the building has double-surface walls with an air-conditioned space between them, and a 19" enclosure with water-cooled recalculating air within +/- 0.2 K was developed. The realized performance, as mentioned above, almost satisfied our demand. All of our effort for instrument development increased the possibility to realize further stable X ray generation at the XFEL.

REFERENCES

[1]   Tanaka, T. & Shintake, T. (Eds) SCSS X-FEL Conceptual Design Report, (RIKEN Harima Institute, Hyogo, Japan, 2005).

[2]   Altarelli, M. et al. (Eds) XFEL: The European X-Ray Free-Electron Laser, Technical Design Report. Preprint DESY 2006-097, (DESY Hamburg, 2006).

[3]   Arthur, J. et al. Linac Coherent Light Source (LCLS) Conceptual Design Report, SLAC-R593 (Stanford, 2002).

[4]   J. Miao et al., PNAS, 98, p. 6641 (2001).

[5]   H. Tanaka, private communication, Internal Report of XFEL/Spring-8.

[6]   T. Shintake et.al., A compact free electron laser generates coherent radiation from extreme ultraviolet to X-rays, Nature, in press, (2008).

[7]   H. Tanaka et al., Operation Status of the SCSS Test Accelerator, proc. of EPAC08, pp 1944-1946, (2008).

[8]   Y. Otake *et al.*, Timing and LLRF System of Japanese XFEL to Realize Femto-second Stability, Proc. of ICALEPCS07, pp 706-710, (2007).

[9]   H. Maesaka et al., Precise RF Control System of SCSS Test Accelerator, proc. of EPAC08, pp 1404-1406, (2008).

[10] T. Shintake and T. Inagaki, private communication.

[11] S. Tahashi et al., Precise Temperature Regulation System for C-Band Accelerating Structure, proc. of APAC04, pp. 678-680, (2004).

[12] J. S. Oh, Stable RF Phase Insensitive to the Modulator Voltage Fluctuation of the C-Band Main Linac for SCSS XFEL, proc. of FEL06, PP 684-687, (2006).

[13] S. Goldman, Frequency Analysis, Modulation and Noise, DOVER, pp 211-215, 1967.

[14] Y. Otake et al., Sub-pico-second trigger system for the SCSS prototype accelerator, Proc. of FEL06, PP 645-648, (2006).